

RESEARCH ARTICLE | JANUARY 29 2025

Residual-ZZ-coupling suppression and fast two-qubit gate for Kerr-cat qubits based on level-degeneracy engineering

Special Collection: [Quantum Networks](#)

Takaaki Aoki  ; Akiyoshi Tomonaga  ; Kosuke Mizuno  ; Shunpei Masuda 

 Check for updates

Appl. Phys. Lett. 126, 044004 (2025)

<https://doi.org/10.1063/5.0241315>



View
Online



Export
Citation

Articles You May Be Interested In

Quantum heat transport of a two-qubit system: Interplay between system-bath coherence and qubit-qubit coherence

J. Chem. Phys. (August 2015)

Josephson devices for controllable flux qubit and interqubit coupling

Appl. Phys. Lett. (October 2005)

Dissipative dynamics in a tunable Rabi dimer with periodic harmonic driving

J. Chem. Phys. (May 2019)

Webinar From Noise to Knowledge

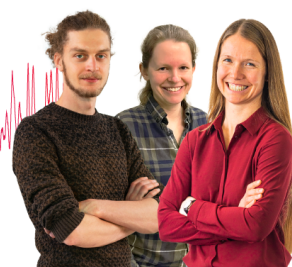
May 13th – Register now



Zurich
Instruments



Universität
Konstanz



Residual-ZZ-coupling suppression and fast two-qubit gate for Kerr-cat qubits based on level-degeneracy engineering

Cite as: Appl. Phys. Lett. **126**, 044004 (2025); doi: [10.1063/5.0241315](https://doi.org/10.1063/5.0241315)

Submitted: 30 September 2024 · Accepted: 17 January 2025 ·

Published Online: 29 January 2025



Takaaki Aoki,^{1,a)} Akiyoshi Tomonaga,^{1,2} Kosuke Mizuno,¹ and Shumpei Masuda^{1,2,b)}

AFFILIATIONS

¹Global Research and Development Center for Business by Quantum-AI Technology (G-QuAT), National Institute of Advanced Industrial Science and Technology (AIST), 1-1-1 Umezono, Tsukuba, Ibaraki 305-8568, Japan

²NEC-AIST Quantum Technology Cooperative Research Laboratory, National Institute of Advanced Industrial Science and Technology (AIST), 1-1-1 Umezono, Tsukuba, Ibaraki 305-8568, Japan

Note: This paper is part of the APL Special Topic, Quantum Networks.

a)Author to whom correspondence should be addressed: takaaki-aoki@aist.go.jp

b)Electronic mail: shumpei.masuda@aist.go.jp

ABSTRACT

Building large-scale quantum computers requires an interqubit-coupling scheme with a high on-off ratio to avoid unwanted crosstalk coming from residual coupling and to enable fast multi-qubit operations. We propose a ZZ-coupling scheme for two Kerr-cat qubits with a frequency-tunable coupler. By making four relevant states of the two Kerr-cat qubits quadruply degenerate, we can switch off the ZZ coupling. By partially lifting the level degeneracy, we can switch it on. We theoretically show that an experimentally feasible circuit model suppresses the residual ZZ coupling. Moreover, our circuit can realize $R_{ZZ}(-\pi/2)$ -gate fidelity higher than 99.9% within 18 ns when decoherence is ignored. Our model includes the first-order terms in expansion beyond the rotating-wave approximation.

© 2025 Author(s). All article content, except where otherwise noted, is licensed under a Creative Commons Attribution-NonCommercial-NoDerivs 4.0 International (CC BY-NC-ND) license (<https://creativecommons.org/licenses/by-nc-nd/4.0/>). <https://doi.org/10.1063/5.0241315>

A Kerr-cat qubit, which stores quantum information on a parametrically (squeeze-)driven Kerr-nonlinear oscillator (KPO),^{1–3} is attracting much attention as a candidate platform for quantum computation. One of its advantages is its biased-noise nature: its logical states are defined as two coherent states with opposite phases, and the bit-flip rate is exponentially suppressed with the mean photon number,⁴ which allows efficient quantum error corrections.⁵ This biased-noise nature comes from a double-well Hamiltonian of a KPO.⁶ To investigate its energy-level structure, the reflection spectroscopy has been studied theoretically⁷ and experimentally.⁸ Energies of an effective static Hamiltonian of a KPO and quasi-energies obtained from Floquet theory have been compared theoretically.⁹ Pairwise level degeneracies owing to increased barrier height of the double well have been observed in experiment.^{6,10} When the detuning of the resonance frequency of a KPO from half the parametric-drive frequency takes specific values, the energy spectrum of the KPO shows multiple degeneracies and bit-flip errors are further suppressed, which has been shown theoretically¹¹ and experimentally.^{12,13} A fully tunable asymmetric double well has been created experimentally.¹⁴

A universal gate set for Kerr-cat qubits can be constructed for example by Z-axis rotations (R_Z gates) with all rotation angles, an X-axis rotation (R_X gate) with rotation angle $-\pi/2$, and a ZZ rotation (R_{ZZ} gate) with rotation angle $-\pi/2$.² Various schemes for gate operations on Kerr-cat qubits have been theoretically studied: an R_Z gate with a single-photon drive;^{2,3} an R_X gate by controlling the oscillator frequency;^{2,3} an R_X gate using time evolution under the Kerr Hamiltonian without the squeezing drive;³ an R_X gate using effective excited states;¹⁵ an R_{ZZ} gate using beam splitter coupling;^{2,3} an R_{ZZ} gate by controlling the phase of the squeezing drive;¹⁶ an R_{ZZ} gate using conditional driving;^{17,18} acceleration of the elementary gates;¹⁹ and nontrivial bias-preserving gates.^{20–22} Gate operations on Kerr-cat qubits have also been experimentally demonstrated: R_Z , R_X ,²³ and $\sqrt{i}\text{SWAP}$ ²⁴ gates using dc superconducting quantum interference devices (SQUIDs); and R_Z and R_X gates using superconducting nonlinear asymmetric inductive elements (SNAILS).^{13,25,26}

An R_{ZZ} gate is based on ZZ coupling between qubits. If we cannot switch off the ZZ coupling, the residual coupling causes crosstalk²⁷ among qubits, yielding unwanted correlations between them. Because

crosstalk errors are difficult to remove with quantum error corrections, which in general depend on errors to be local,²⁷ a scheme without residual coupling is desired to build a large-scale quantum computer. In order to suppress residual coupling, tunable couplers have been utilized in transmon systems,^{28–40} which also enable fast multi-qubit operations. In Ref. 41, the authors have developed a coupling scheme for two Kerr-cat qubits in which two tunable resonators are used as couplers and the frequency of a resonator is controlled. Although the scheme can suppress the residual coupling, a simpler scheme with less residual coupling is desirable.

In this Letter, we propose a coupling scheme for two Kerr-cat qubits with a better performance using a single tunable resonator as a coupler. By tuning the coupler frequency, we engineer the degeneracy of four relevant states of the two Kerr-cat qubits. This allows a cancellation of the residual ZZ coupling and a fast and high-fidelity R_{ZZ} gate. We show a circuit model that is experimentally feasible and numerically investigate its performance. Our Hamiltonian derived from the circuit model incorporates the first-order terms in expansion beyond the rotating-wave approximation (RWA). We use two coherent states with opposite phases as the computational basis of a Kerr-cat qubit in this Letter, although their superpositions are also used as computational basis in other papers.

Before discussing the scheme for Kerr-cat qubits, we explain the relation between ZZ coupling and energy-level degeneracy of a diagonalized two-qubit Hamiltonian. The Hamiltonian is given by

$$\hat{H}_{2q} = \sum_{l,m=0}^1 E_{l,m} |\psi_{l,m}\rangle\langle\psi_{l,m}| = \begin{pmatrix} E_{0,0} & 0 & 0 & 0 \\ 0 & E_{0,1} & 0 & 0 \\ 0 & 0 & E_{1,0} & 0 \\ 0 & 0 & 0 & E_{1,1} \end{pmatrix}, \quad (1)$$

where $\{|\psi_{l,m}\rangle |l, m \in \{0, 1\}\}$ are four eigenstates and form an orthonormal basis; $E_{l,m}$ is the eigenenergy of eigenstate $|\psi_{l,m}\rangle$. This Hamiltonian can be rewritten as

$$\hat{H}_{2q}/\hbar = \frac{\zeta_{II}}{4} \hat{I}\hat{I} + \frac{\zeta_{ZZ}}{4} \hat{Z}\hat{Z} + \frac{\zeta_{ZI}}{4} \hat{Z}\hat{I} + \frac{\zeta_{IZ}}{4} \hat{I}\hat{Z}, \quad (2)$$

where

$$\hbar\zeta_{II} = E_{0,0} + E_{0,1} + E_{1,0} + E_{1,1}, \quad (3)$$

$$\hbar\zeta_{ZZ} = E_{0,0} - E_{0,1} - E_{1,0} + E_{1,1}, \quad (4)$$

$$\hbar\zeta_{ZI} = E_{0,0} + E_{0,1} - E_{1,0} - E_{1,1}, \quad (5)$$

$$\hbar\zeta_{IZ} = E_{0,0} - E_{0,1} + E_{1,0} - E_{1,1}, \quad (6)$$

$$\hat{I} = \begin{pmatrix} 1 & 0 \\ 0 & 1 \end{pmatrix}, \quad \hat{Z} = \begin{pmatrix} 1 & 0 \\ 0 & -1 \end{pmatrix}, \quad (7)$$

and $\hbar = h/(2\pi)$ is the reduced Planck constant. ζ_{ZZ} in Eq. (4) is a ZZ-coupling strength.^{30–40} Our strategy to cancel ZZ coupling, $\zeta_{ZZ} = 0$, is to make the four eigenstates quadruply degenerate by tuning system parameters, which also leads to $\zeta_{ZI} = 0$ and $\zeta_{IZ} = 0$. We define four logical states $\{|\widetilde{l}, m\rangle |l, m \in \{0, 1\}\}$ as the quadruply degenerate eigenstates.

On the other hand, if we retain the degeneracy between $|\psi_{0,0}\rangle$ and $|\psi_{1,1}\rangle$ and that between $|\psi_{0,1}\rangle$ and $|\psi_{1,0}\rangle$ while partially lifting the degeneracy between the former two states and the latter two, we can

perform only an R_{ZZ} gate as follows. We assume that at $t = 0$, ZZ coupling is switched off, $\zeta_{ZZ}(0) = 0$. We prepare the initial state as

$$|\Psi(0)\rangle = \sum_{l,m=0}^1 \beta_{l,m} |\widetilde{l}, m\rangle, \quad (8)$$

where $\beta_{l,m}$ is a coefficient. When the system parameters are changed adiabatically with the condition $\zeta_{ZZ}(t_g) = 0$, where t_g is the gate time, the state of the system at $t = t_g$ becomes

$$\begin{aligned} |\Psi(t_g)\rangle &= \mathcal{T} \exp\left(-\frac{i}{\hbar} \int_0^{t_g} \hat{H}_{2q}(t) dt\right) |\Psi(0)\rangle \\ &= e^{-i\theta} \hat{R}_{ZZ}(\Theta) |\Psi(0)\rangle =: e^{-i\theta} |\Psi_\Theta^{\text{ideal}}\rangle, \end{aligned} \quad (9)$$

where \mathcal{T} is the time-ordering operator,

$$\theta := \int_0^{t_g} \frac{\zeta_{II}(t)}{4} dt \quad (10)$$

is a global phase, and

$$\begin{aligned} \hat{R}_{ZZ}(\Theta) &= \sum_{l,m=0}^1 e^{-i(2\delta_{l,m}-1)\Theta/2} |\widetilde{l}, m\rangle \langle \widetilde{l}, m| \\ &= \begin{pmatrix} e^{-i\Theta/2} & 0 & 0 & 0 \\ 0 & e^{i\Theta/2} & 0 & 0 \\ 0 & 0 & e^{i\Theta/2} & 0 \\ 0 & 0 & 0 & e^{-i\Theta/2} \end{pmatrix}, \end{aligned} \quad (11)$$

with

$$\Theta := \int_0^{t_g} \frac{\zeta_{ZZ}(t)}{2} dt \quad (12)$$

being the rotation angle and $\delta_{l,m}$ being the Kronecker delta. Here, we have ignored decoherence. In reality, some unwanted nonadiabatic transitions are unavoidable, and the second equal sign in Eq. (9) is replaced by an approximately equal one. For evaluation of the degree of approximation, we later calculate gate fidelity. We show a schematic of our level-degeneracy engineering in Fig. 1.

Now, we introduce the level-degeneracy engineering for Kerr-cat qubits. We consider a system consisting of two Kerr parametric oscillators^{2,3} (KPOs, subsystems 1 and 2) and a tunable resonator (subsystem c). This system constitutes two Kerr-cat qubits. A circuit model of our system is shown in Fig. 2. The center of each SQUID of subsystem $\lambda \in \{1, 2, c\}$ is threaded by a magnetic flux $\tilde{\Phi}_\lambda(t)$. We decompose a dimensionless magnetic flux $\tilde{\varphi}_\lambda(t) := \tilde{\Phi}_\lambda(t)/\phi_0$, where $\phi_0 = \hbar/(2e)$ is the reduced flux quantum [$\hbar/(2e)$ is the flux quantum], into bias and pump parts as⁴³

$$\tilde{\varphi}_\lambda(t) = \tilde{\varphi}_\lambda^{\text{bias}}(t) + \tilde{\varphi}_\lambda^{\text{pump}}(t), \quad (13)$$

$$\tilde{\varphi}_\lambda^{\text{pump}}(t) = -2\pi\varepsilon_{p,\lambda} \cos(\omega_p t), \quad (14)$$

with $\varepsilon_{p,j} \ll 1$ for $j \in \{1, 2\}$ and $\varepsilon_{p,c} = 0$. In the laboratory frame, the KPOs are parametrically pumped at frequency ω_p but the resonator is not. The bias parts $\{\tilde{\varphi}_\lambda^{\text{bias}}(t)\}$ are the key components for the level-degeneracy engineering. At first, we assume that they are time

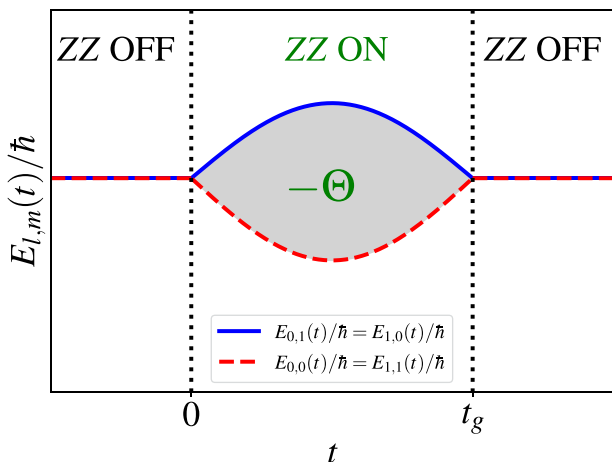


FIG. 1. A schematic of our level-degeneracy engineering to control ZZ coupling. An $R_{ZZ}(\Theta)$ gate is applied for $0 \leq t \leq t_g$. The light gray area is $-\Theta$.

independent; $\tilde{\varphi}_\lambda^{\text{bias}}(t) = \tilde{\varphi}_\lambda^{\text{bias}}(0) = \tilde{\varphi}_\lambda^{\text{bias}} \forall t$. The effective Hamiltonian \hat{H} of our system is written as (see the [supplementary material](#))

$$\hat{H} = \sum_{j=1,2} \hat{H}_j + \hat{H}_c + \hat{H}_I, \quad (15)$$

$$\begin{aligned} \hat{H}_j/\hbar = & -\frac{\tilde{K}_j}{2} \hat{a}_j^{\dagger 2} \hat{a}_j^2 + \frac{\tilde{p}_j}{2} (\hat{a}_j^{\dagger 2} + \hat{a}_j^2) + \tilde{\Delta}_j \hat{a}_j^\dagger \hat{a}_j \\ & - \frac{17K_j^2}{18\omega_p} \hat{a}_j^{\dagger 3} \hat{a}_j^3 + \frac{5K_j p_j}{6\omega_p} (\hat{a}_j^{\dagger 3} \hat{a}_j + \hat{a}_j^\dagger \hat{a}_j^3), \end{aligned} \quad (16)$$

$$\hat{H}_c/\hbar = -\frac{\tilde{K}_c}{2} \hat{a}_c^{\dagger 2} \hat{a}_c^2 + \tilde{\Delta}_c \hat{a}_c^\dagger \hat{a}_c - \frac{17K_c^2}{18\omega_p} \hat{a}_c^{\dagger 3} \hat{a}_c^3, \quad (17)$$

$$\begin{aligned} \hat{H}_I/\hbar = & \sum_{j=1,2} \tilde{g}_{jc} (\hat{a}_j^\dagger \hat{a}_c + \hat{a}_j \hat{a}_c^\dagger) + \tilde{g}_{12} (\hat{a}_1^\dagger \hat{a}_2 + \hat{a}_1 \hat{a}_2^\dagger) \\ & - \sum_{j=1,2} \frac{g_{jc}}{\omega_p} \left[K_j (\hat{a}_j^{\dagger 2} \hat{a}_j \hat{a}_c + \hat{a}_j^\dagger \hat{a}_j^2 \hat{a}_c^\dagger) \right. \\ & \left. - p_j (\hat{a}_j^\dagger \hat{a}_c^\dagger + \hat{a}_j \hat{a}_c) + K_c (\hat{a}_j^\dagger \hat{a}_c^\dagger \hat{a}_c^2 + \hat{a}_j \hat{a}_c^{\dagger 2} \hat{a}_c) \right] \\ & - \frac{g_{12}}{\omega_p} \left[K_1 (\hat{a}_1^{\dagger 2} \hat{a}_1 \hat{a}_2 + \hat{a}_1^\dagger \hat{a}_1^2 \hat{a}_2^\dagger) \right. \\ & \left. + K_2 (\hat{a}_1^\dagger \hat{a}_2^\dagger \hat{a}_2^2 + \hat{a}_1 \hat{a}_2^{\dagger 2} \hat{a}_2) - (p_1 + p_2) (\hat{a}_1^\dagger \hat{a}_2^\dagger + \hat{a}_1 \hat{a}_2) \right], \end{aligned} \quad (18)$$

where \hat{H}_λ is the Hamiltonian of subsystem $\lambda \in \{1, 2, c\}$ and \hat{H}_I is the interaction Hamiltonian; \hat{a}_λ is the annihilation operator of subsystem $\lambda \in \{1, 2, c\}$. The parameters with tilde incorporate the effect of the first-order terms in expansion beyond the rotating-wave approximation, see the [supplementary material](#); K_λ is the Kerr nonlinearity of subsystem $\lambda \in \{1, 2, c\}$; p_j is the amplitude of the parametric drive of subsystem $j \in \{1, 2\}$; Δ_λ is the detuning of the dressed resonance frequency ω_λ of subsystem $\lambda \in \{1, 2, c\}$ from $\omega_p/2$, that is, $\Delta_\lambda = \omega_\lambda - \omega_p/2$; $g_{\lambda\lambda'}$ is the coupling strength between subsystems λ and λ' ($\lambda, \lambda' \in \{1, 2, c\}$). The above parameters are tuned through

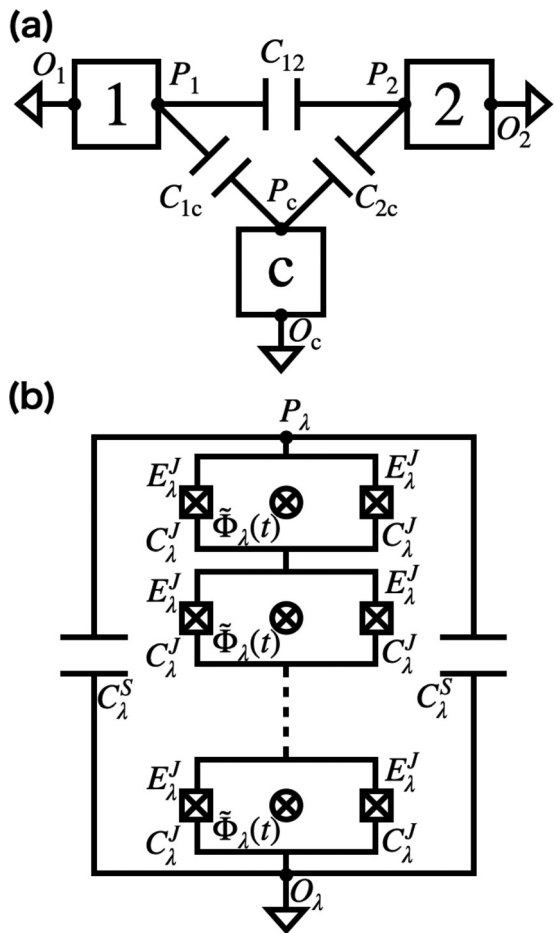


FIG. 2. A circuit model of our system, which constitutes two Kerr-cat qubits. (a) Subsystems 1, 2, and c are coupled capacitively. (b) A circuit diagram of subsystem $\lambda \in \{1, 2, c\}$, which comprises two identical shunting capacitors of capacitance C_λ^S and an array of N_λ identical symmetric dc SQUIDS each of which has two Josephson junctions of Josephson energy E_λ^J and capacitance C_λ^J . It is connected to the ground via node O_λ . It is symmetric with respect to the line through P_λ and O_λ . The center of each SQUID is threaded by a magnetic flux $\tilde{\Phi}_\lambda(t)$ into the paper.⁴²

$\{\tilde{\varphi}_\lambda^{\text{bias}}\}$ as shown in the [supplementary material](#). We note that although K_c and \tilde{K}_c are not essential for our scheme, we include them in our Hamiltonian to make our model realistic, because a tunable resonator actually has Kerr nonlinearity; see, for example, Sec. II B 1 in Ref. 44. In the literature on KPOs, as a Hamiltonian of a KPO, a simpler form, which is derived using the rotating-wave approximation and contains only the first line in Eq. (16) without tilde, is often used. However, when the Kerr nonlinearity is large, the discrepancy between the simple Hamiltonian and a Hamiltonian considering counter-rotating terms, which are omitted in the rotating-wave approximation, cannot be neglected.^{9,14,45,46} This is why we have included the first-order terms in expansion beyond the rotating-wave approximation; see the [supplementary material](#).

Hamiltonian \hat{H} can be rewritten as

$$\hat{H} = \hat{H}_0 + \hat{H}_{ZZ} + \sum_{j=1,2} \hat{H}_{X_j}, \quad (19)$$

$$\begin{aligned} \hat{H}_0/\hbar &= \sum_{j=1,2} \left[-\frac{\tilde{K}_j}{2} \left(\hat{a}_j^{\dagger 2} - \tilde{\alpha}_j^2 \right) \left(\hat{a}_j^2 - \tilde{\alpha}_j^2 \right) + \frac{\tilde{K}_j}{2} \tilde{\alpha}_j^4 \right] \\ &\quad + \tilde{\Delta}_c \left(\hat{a}_c^{\dagger} + \frac{\tilde{g}_{1c}}{\tilde{\Delta}_c} \hat{a}_1^{\dagger} + \frac{\tilde{g}_{2c}}{\tilde{\Delta}_c} \hat{a}_2^{\dagger} \right) \\ &\quad \times \left(\hat{a}_c + \frac{\tilde{g}_{1c}}{\tilde{\Delta}_c} \hat{a}_1 + \frac{\tilde{g}_{2c}}{\tilde{\Delta}_c} \hat{a}_2 \right), \end{aligned} \quad (20)$$

$$\begin{aligned} \hat{H}_{ZZ}/\hbar &= \left(\tilde{g}_{12} - \frac{\tilde{g}_{1c}\tilde{g}_{2c}}{\tilde{\Delta}_c} \right) (\hat{a}_1^{\dagger}\hat{a}_2 + \hat{a}_1\hat{a}_2^{\dagger}) \\ &\quad - \frac{\tilde{K}_c}{2} \hat{a}_c^{\dagger 2} \hat{a}_c^2 - \frac{17K_c^2}{18\omega_p} \hat{a}_c^{\dagger 3} \hat{a}_c^3 \\ &\quad - \sum_{j=1,2} \frac{g_{jc}}{\omega_p} \left[K_j (\hat{a}_j^{\dagger 2} \hat{a}_j \hat{a}_c + \hat{a}_j^{\dagger} \hat{a}_j^2 \hat{a}_c^{\dagger}) \right. \\ &\quad \left. - p_j (\hat{a}_j^{\dagger} \hat{a}_c^{\dagger} + \hat{a}_j \hat{a}_c) + K_c (\hat{a}_j^{\dagger} \hat{a}_c^{\dagger} \hat{a}_c^2 + \hat{a}_j \hat{a}_c^{\dagger 2} \hat{a}_c) \right] \\ &\quad - \frac{g_{12}}{\omega_p} \left[K_1 (\hat{a}_1^{\dagger 2} \hat{a}_1 \hat{a}_2 + \hat{a}_1^{\dagger} \hat{a}_1^2 \hat{a}_2^{\dagger}) \right. \\ &\quad \left. + K_2 (\hat{a}_1^{\dagger} \hat{a}_2^{\dagger} \hat{a}_2^2 + \hat{a}_1 \hat{a}_2^{\dagger 2} \hat{a}_2) \right. \\ &\quad \left. - (p_1 + p_2) (\hat{a}_1^{\dagger} \hat{a}_2^{\dagger} + \hat{a}_1 \hat{a}_2) \right], \end{aligned} \quad (21)$$

$$\hat{H}_{X_j}/\hbar = \left(\tilde{\Delta}_j - \frac{\tilde{g}_{jc}^2}{\tilde{\Delta}_c} \right) \hat{a}_j^{\dagger} \hat{a}_j - \frac{17K_j^2}{18\omega_p} \hat{a}_j^{\dagger 3} \hat{a}_j^3 + \frac{5K_j p_j}{6\omega_p} (\hat{a}_j^{\dagger 3} \hat{a}_j + \hat{a}_j^{\dagger} \hat{a}_j^3), \quad (22)$$

where $\tilde{\alpha}_j := \sqrt{\tilde{p}_j/\tilde{K}_j}$, \hat{H}_{ZZ} is a ZZ-coupling Hamiltonian, and \hat{H}_{X_j} is a Hamiltonian for R_X gates on the j th Kerr-cat qubit. The tensor products of coherent states of subsystems 1, 2, and c given by

$$|\psi_{0,0}\rangle := |\tilde{\alpha}_1, \tilde{\alpha}_2, -\tilde{\alpha}_c^+\rangle, \quad (23)$$

$$|\psi_{0,1}\rangle := |\tilde{\alpha}_1, -\tilde{\alpha}_2, -\tilde{\alpha}_c^-\rangle, \quad (24)$$

$$|\psi_{1,0}\rangle := |-\tilde{\alpha}_1, \tilde{\alpha}_2, \tilde{\alpha}_c^-\rangle, \quad (25)$$

$$|\psi_{1,1}\rangle := |-\tilde{\alpha}_1, -\tilde{\alpha}_2, \tilde{\alpha}_c^+\rangle, \quad (26)$$

with

$$\tilde{\alpha}_c^{\pm} = \frac{\tilde{g}_{1c}\tilde{\alpha}_1 \pm \tilde{g}_{2c}\tilde{\alpha}_2}{\tilde{\Delta}_c}, \quad (27)$$

are quadruply degenerate eigenstates of \hat{H}_0 with eigenenergy $E_0 = \hbar \sum_{j=1,2} \tilde{K}_j \tilde{\alpha}_j^4 / 2$. These four states are almost orthogonal since the inner product of two coherent states with opposite phases is exponentially small; $|\langle \tilde{\alpha} | -\tilde{\alpha} \rangle| = e^{-2\tilde{\alpha}}$. We set $\tilde{\alpha}_j \approx 2$ so that $|\langle \tilde{\alpha}_j | -\tilde{\alpha}_j \rangle| \approx 3 \times 10^{-4}$ for $j \in \{1, 2\}$. In order not to apply unwanted R_X gates, we impose $\langle \tilde{\alpha}_j | \hat{H}_{X_j} | \tilde{\alpha}_j \rangle = 0$, that is

$$\tilde{\Delta}_j = \frac{\tilde{g}_{jc}^2}{\tilde{\Delta}_c} + \frac{17K_j^2}{18\omega_p} \tilde{\alpha}_j^4 - \frac{5K_j p_j}{6\omega_p} \tilde{\alpha}_j^2, \quad (28)$$

for $j \in \{1, 2\}$. Since ω_p is much larger than the other parameters, the terms proportional to $1/\omega_p$ in \hat{H}_{ZZ} can be treated as perturbations to

\hat{H}_0 . By tuning $\tilde{\Delta}_c$, we set $\tilde{g}_{12} - \tilde{g}_{1c}\tilde{g}_{2c}/\tilde{\Delta}_c$ so small that the first term in \hat{H}_{ZZ} can be treated as a perturbation. We also set $K_c \ll K_j$ and $|\tilde{\alpha}_c^{\pm}| \ll \tilde{\alpha}_j$ so that the second term in \hat{H}_{ZZ} can be treated as a perturbation. Then, \hat{H}_{ZZ} itself can be treated as a perturbation. In the first order of perturbation, the four eigenenergies are calculated as follows:

$$\begin{aligned} E_{0,0}^{(1)}/\hbar &= E_{1,1}^{(1)}/\hbar \\ &= E_0/\hbar + 2 \left(\tilde{g}_{12} - \frac{\tilde{g}_{1c}\tilde{g}_{2c}}{\tilde{\Delta}_c} \right) \tilde{\alpha}_1 \tilde{\alpha}_2 \\ &\quad - \frac{\tilde{K}_c}{2} (\tilde{\alpha}_c^+)^4 - \frac{17K_c^2}{18\omega_p} (\tilde{\alpha}_c^+)^6 \\ &\quad + \sum_{j=1,2} \frac{2g_{jc}}{\omega_p} \left[K_j \tilde{\alpha}_j^3 \tilde{\alpha}_c^+ - p_j \tilde{\alpha}_j \tilde{\alpha}_c^+ + K_c \tilde{\alpha}_j (\tilde{\alpha}_c^+)^3 \right] \\ &\quad - \frac{2g_{12}}{\omega_p} \left[K_1 \tilde{\alpha}_1^3 \tilde{\alpha}_2 + K_2 \tilde{\alpha}_1 \tilde{\alpha}_2^3 - (p_1 + p_2) \tilde{\alpha}_1 \tilde{\alpha}_2 \right], \end{aligned} \quad (29)$$

$$\begin{aligned} E_{0,1}^{(1)}/\hbar &= E_{1,0}^{(1)}/\hbar \\ &= E_0/\hbar - 2 \left(\tilde{g}_{12} - \frac{\tilde{g}_{1c}\tilde{g}_{2c}}{\tilde{\Delta}_c} \right) \tilde{\alpha}_1 \tilde{\alpha}_2 \\ &\quad - \frac{\tilde{K}_c}{2} (\tilde{\alpha}_c^-)^4 - \frac{17K_c^2}{18\omega_p} (\tilde{\alpha}_c^-)^6 \\ &\quad + \sum_{j=1,2} \frac{2(-1)^{j+1}g_{jc}}{\omega_p} \left[K_j \tilde{\alpha}_j^3 \tilde{\alpha}_c^- - p_j \tilde{\alpha}_j \tilde{\alpha}_c^- + K_c \tilde{\alpha}_j (\tilde{\alpha}_c^-)^3 \right] \\ &\quad + \frac{2g_{12}}{\omega_p} \left[K_1 \tilde{\alpha}_1^3 \tilde{\alpha}_2 + K_2 \tilde{\alpha}_1 \tilde{\alpha}_2^3 - (p_1 + p_2) \tilde{\alpha}_1 \tilde{\alpha}_2 \right], \end{aligned} \quad (30)$$

where the superscript (1) denotes the first order of perturbation. Substituting these four eigenenergies into Eqs. (4)–(6), we obtain

$$\begin{aligned} \zeta_{ZZ}^{(1)} &= 8 \left(\tilde{g}_{12} - \frac{\tilde{g}_{1c}\tilde{g}_{2c}}{\tilde{\Delta}_c} \right) \tilde{\alpha}_1 \tilde{\alpha}_2 - \tilde{K}_c \left[(\tilde{\alpha}_c^+)^4 - (\tilde{\alpha}_c^-)^4 \right] \\ &\quad - \frac{17K_c^2}{9\omega_p} \left[(\tilde{\alpha}_c^+)^6 - (\tilde{\alpha}_c^-)^6 \right] \\ &\quad + \sum_{j=1,2} \frac{4g_{jc}}{\omega_p} \left[K_j \tilde{\alpha}_j^3 \tilde{\alpha}_c^+ - p_j \tilde{\alpha}_j \tilde{\alpha}_c^+ + K_c \tilde{\alpha}_j (\tilde{\alpha}_c^+)^3 \right] \\ &\quad - \sum_{j=1,2} \frac{4(-1)^{j+1}g_{jc}}{\omega_p} \\ &\quad \times \left[K_j \tilde{\alpha}_j^3 \tilde{\alpha}_c^- - p_j \tilde{\alpha}_j \tilde{\alpha}_c^- + K_c \tilde{\alpha}_j (\tilde{\alpha}_c^-)^3 \right] \\ &\quad - \frac{8g_{12}}{\omega_p} \left[K_1 \tilde{\alpha}_1^3 \tilde{\alpha}_2 + K_2 \tilde{\alpha}_1 \tilde{\alpha}_2^3 - (p_1 + p_2) \tilde{\alpha}_1 \tilde{\alpha}_2 \right], \end{aligned} \quad (31)$$

and $\zeta_{ZI}^{(1)} = \zeta_{IZ}^{(1)} = 0$. We can cancel $\zeta_{ZZ}^{(1)}$ by regulating $\tilde{\varphi}_c^{\text{bias}}$ as in Fig. 3.

In order to check whether the above scheme for canceling residual ZZ coupling based on the first order of perturbation is effective, we numerically calculate infidelity $1 - |\langle \Psi(t) | \Psi(0) \rangle|^2$, where $|\Psi(t)\rangle = e^{-i\hat{H}t/\hbar} |\Psi(0)\rangle$ with \hat{H} in Eq. (15) and $|\Psi(0)\rangle$ in Eq. (8) with $\beta_{0,0} = \beta_{0,1} = \beta_{1,0} = \beta_{1,1}$. For numerical calculations in this Letter, we use Quantum Toolbox in Python (QuTiP).^{47,48} Aiming to satisfy $\zeta_{ZZ}^{(1)}/2\pi = 0$ kHz [Eq. (31)] and Eq. (28), we choose the parameter values in Table I. We can suppress the residual coupling so that the

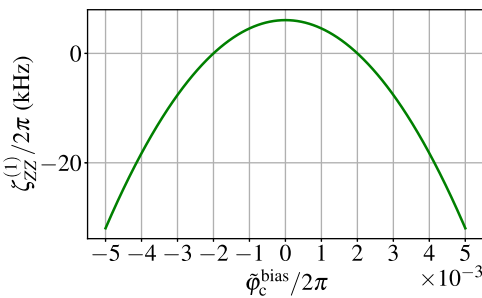


FIG. 3. $\zeta_{ZZ}^{(1)}$ as a function of $\tilde{\varphi}_c^{bias}$. We have $\zeta_{ZZ}^{(1)} / 2\pi = 0$ kHz when $\tilde{\varphi}_c^{bias} / 2\pi \approx \pm 2 \times 10^{-3}$. The relation between $\tilde{\varphi}_c^{bias}$ and system parameters are given in the [supplementary material](#). Values of the parameters unrelated to $\tilde{\varphi}_c^{bias}$ are set as in [Table I](#).

TABLE I. Parameter values chosen to satisfy $\zeta_{ZZ}^{(1)} / 2\pi = 0$ kHz [Eq. (31)] and Eq. (28), although there is a slight deviation from Eq. (28) as at the bottom. The bold values in the left side are design values, from which the other values in the right side are calculated.

$C_1^S = C_2^S$ (fF)	170	$K_1 / 2\pi$ (MHz)	13.0
$C_1^J = C_2^J$ (fF)	30	$K_2 / 2\pi$ (MHz)	13.0
$N_1 = N_2$	2	$K_c / 2\pi$ (MHz)	1.48
C_c^S (fF)	400	$\omega_1 / 2\pi$ (GHz)	9.997
C_c^J (fF)	30	$\omega_2 / 2\pi$ (GHz)	9.996
N_c	4	$\omega_c / 2\pi$ (GHz)	10.4
C_{1c} (fF)	2.5	$p_1 / 2\pi$ (MHz)	55.1
C_{2c} (fF)	1.3	$p_2 / 2\pi$ (MHz)	55.2
C_{12} (fF)	0.05	$g_{1c} / 2\pi$ (MHz)	23.1
E_1^J / h (GHz)	341	$g_{2c} / 2\pi$ (MHz)	12.0
E_2^J / h (GHz)	340	$g_{12} / 2\pi$ (kHz)	726
E_c^J / h (THz)	1.14	$\tilde{K}_1 / 2\pi$ (MHz)	13.1
$\tilde{\varphi}_1^{bias} / 2\pi$	0.250323	$\tilde{K}_2 / 2\pi$ (MHz)	13.1
$\tilde{\varphi}_2^{bias} / 2\pi$	0.250472	$\tilde{K}_c / 2\pi$ (MHz)	1.48
$\tilde{\varphi}_c^{bias} / 2\pi$	2×10^{-3}	$\tilde{p}_1 / 2\pi$ (MHz)	55.2
$\varepsilon_{p,1} = \varepsilon_{p,2}$	7×10^{-3}	$\tilde{p}_2 / 2\pi$ (MHz)	55.3
$\varepsilon_{p,c}$	0	$\tilde{\Delta}_1 / 2\pi$ (MHz)	1.25
$\omega_p / 2\pi$ (GHz)	19.990741	$\tilde{\Delta}_2 / 2\pi$ (kHz)	257
$\kappa / 2\pi$ (kHz)	4 or 0	$\tilde{\Delta}_c / 2\pi$ (MHz)	389
		$\tilde{g}_{1c} / 2\pi$ (MHz)	23.1
		$\tilde{g}_{2c} / 2\pi$ (MHz)	12.0
		$\tilde{g}_{12} / 2\pi$ (kHz)	711
		$\tilde{\alpha}_1$	2.06
		$\tilde{\alpha}_2$	2.05
		$\tilde{\alpha}_c^+$	0.185
		$\tilde{\alpha}_c^-$	0.058
$\tilde{\Delta}_1 / 2\pi - \left[\frac{\tilde{g}_{1c}^2}{\tilde{\Delta}_c} + \frac{17K_1^2}{18\omega_p} \tilde{\alpha}_1^4 - \frac{5K_1 p_1}{6\omega_p} \tilde{\alpha}_1^2 \right] / 2\pi$ (kHz)			-1.28
$\tilde{\Delta}_2 / 2\pi - \left[\frac{\tilde{g}_{2c}^2}{\tilde{\Delta}_c} + \frac{17K_2^2}{18\omega_p} \tilde{\alpha}_2^4 - \frac{5K_2 p_2}{6\omega_p} \tilde{\alpha}_2^2 \right] / 2\pi$ (kHz)			-3.77

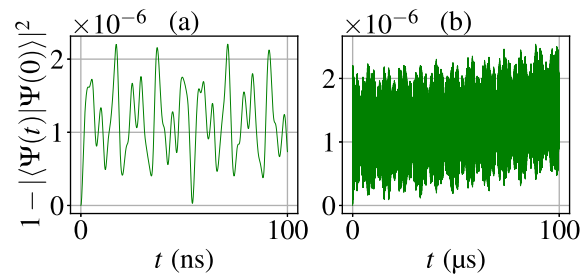


FIG. 4. Infidelity $1 - |\langle \Psi(t) | \Psi(0) \rangle|^2$ when the ZZ coupling should be switched off for (a) $0 \text{ ns} \leq t \leq 100 \text{ ns}$ and (b) $0 \mu\text{s} \leq t \leq 100 \mu\text{s}$. $|\Psi(t)\rangle = e^{-iHt/\hbar}|\Psi(0)\rangle$ with H in Eq. (15) and $|\Psi(0)\rangle$ in Eq. (8) with $\beta_{0,0} = \beta_{0,1} = \beta_{1,0} = \beta_{1,1}$. The parameters used are listed in [Table I](#).

infidelity oscillates and is less than 3×10^{-6} for $0 \mu\text{s} \leq t \leq 100 \mu\text{s}$ as in Fig. 4, about three orders of magnitude smaller than that using two tunable resonators in Ref. 41.

Next, we partially lift the level degeneracy to switch on the ZZ coupling. The bias parts $\{\tilde{\varphi}_\lambda^{bias}(t)\}$ are time dependent and so are the related parameters (see the [supplementary material](#)). Though we can apply an $R_{ZZ}(\Theta)$ gate with arbitrary rotation angle Θ , we here evaluate the performance of the $R_{ZZ}(-\pi/2)$ gate. We tune $\{\tilde{\varphi}_\lambda^{bias}(t)\}$ to satisfy²

$$\tilde{g}_{12} - \frac{\tilde{g}_{1c}\tilde{g}_{2c}}{\tilde{\Delta}_c(t)} = \tilde{g}_{12} - \frac{\tilde{g}_{1c}\tilde{g}_{2c}}{\tilde{\Delta}_c} - \frac{\pi^2}{16\tilde{\alpha}_1\tilde{\alpha}_2 t_g} \sin\left(\frac{\pi t}{t_g}\right) \quad (0 \leq t \leq t_g) \quad (32)$$

and the time-dependent version of Eq. (28) given by

$$\tilde{\Delta}_j(t) = \frac{\tilde{g}_{jc}^2}{\tilde{\Delta}_c(t)} + \frac{17K_j^2}{18\omega_p} \tilde{\alpha}_j^4 - \frac{5K_j p_j}{6\omega_p} \tilde{\alpha}_j^2 \quad (33)$$

with the parameters in [Table I](#). For example, when $t_g = 18 \text{ ns}$, $\{\tilde{\Delta}_\lambda(t)\}$ varies as in Figs. 5(a) and 5(b). We numerically calculate the infidelity of the $R_{ZZ}(-\pi/2)$ gate using

$$1 - \langle \Psi_{-\pi/2}^{\text{ideal}} | \hat{\rho}(t_g) | \Psi_{-\pi/2}^{\text{ideal}} \rangle, \quad (34)$$

where $\hat{\rho}(t)$ is the density operator of the system and the initial state is $|\Psi(0)\rangle$ in Eq. (8) with $\beta_{0,0} = \beta_{0,1} = \beta_{1,0} = \beta_{1,1}$. We assume a single-photon loss for each subsystem as a major source of decoherence. Then, $\hat{\rho}(t)$ obeys the following Gorini-Kossakowski-Sudarshan-Lindblad (GKSL)-type Markovian master equation:^{49,50}

$$\begin{aligned} \frac{d\hat{\rho}(t)}{dt} = & -\frac{i}{\hbar} [\hat{H}(t), \hat{\rho}(t)] \\ & + \kappa \sum_{\lambda=1,2,c} \left(\hat{a}_\lambda \hat{\rho}(t) \hat{a}_\lambda^\dagger - \frac{1}{2} \{ \hat{a}_\lambda^\dagger \hat{a}_\lambda, \hat{\rho}(t) \} \right), \end{aligned} \quad (35)$$

where κ is the single-photon loss rate; $[\bullet, \circ]$ is the commutator; and $\{\bullet, \circ\}$ is the anticommutator.

When the decoherence can be neglected ($\kappa = 0 \text{ Hz}$), the infidelity, which corresponds to green circles in Fig. 5(c), tends to decrease accompanied by oscillation with t_g . We attribute this decrease to the mitigation of unwanted nonadiabatic transitions. The infidelity is less than 10^{-3} for $t_g = 18 \text{ ns}$. We also consider a simpler control in which

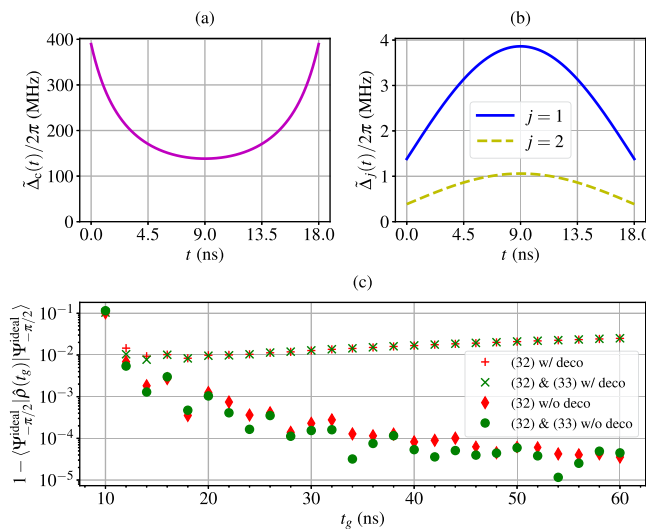


FIG. 5. Time variations of (a) $\tilde{\Delta}_c(t)$, (b) $\tilde{\Delta}_1(t)$, and $\tilde{\Delta}_2(t)$ to satisfy Eqs. (32) and (33) when an $R_{ZZ}(-\pi/2)$ gate is performed with $t_g = 18$ ns. (c) Infidelity of the $R_{ZZ}(-\pi/2)$ gate in Eq. (34). The green circles (Xs) are obtained when all $\tilde{\varphi}_c^{\text{bias}}(t)$, $\tilde{\varphi}_1^{\text{bias}}(t)$, and $\tilde{\varphi}_2^{\text{bias}}(t)$ are tuned to satisfy Eqs. (32) and (33) with $\kappa = 0$ Hz ($\kappa/2\pi = 4$ kHz). The red diamonds (plus signs) are obtained when only $\tilde{\varphi}_c^{\text{bias}}(t)$ is tuned to satisfy Eq. (32) with $\kappa = 0$ Hz ($\kappa/2\pi = 4$ kHz); $\tilde{\varphi}_j^{\text{bias}}(t) = \tilde{\varphi}_c^{\text{bias}}$ $\forall t$ for $j \in \{1, 2\}$ and Eq. (33) is not satisfied. The parameters used are listed in Table I.

only Eq. (32) is satisfied by tuning only $\tilde{\varphi}_c^{\text{bias}}(t)$. The infidelity in this case corresponds to red diamonds in Fig. 5(c). Though worse than the green circles at most of the gate times, the infidelity is also less than 10^{-3} for $t_g = 18$ ns. When $\kappa/2\pi = 4$ kHz, the infidelities of both controls are almost identical. The infidelity is approximately 10^{-2} for $14 \text{ ns} \leq t_g \leq 24$ ns.

In conclusion, we have proposed a ZZ-coupling scheme for two Kerr-cat qubits using a tunable resonator. By engineering the degeneracy of the four relevant states of the two Kerr-cat qubits, we can switch on and off the ZZ coupling. Our scheme is simpler and achieves smaller residual coupling than the scheme using two tunable resonators in Ref. 41. This is because our scheme focuses on energy levels of the whole system, while the scheme in Ref. 41 focuses on those of the effective Hamiltonian of the two resonators; thus, our scheme enables more precise control of ZZ coupling. Our scheme can also be applied to superconducting nonlinear asymmetric inductive element (SNAIL)⁵¹-based Kerr-cat qubits^{13,25,26} with modification of the Hamiltonian. Integrating our scheme with surface codes for biased noise^{52,53} will be an interesting future work.

See the [supplementary material](#) for the derivation of the system Hamiltonian.

The authors are grateful to Hayato Goto for useful discussions. This Letter is based on results obtained from a project (No. JPNP16007), commissioned by the New Energy and Industrial Technology Development Organization (NEDO), Japan. S.M. acknowledges the support from JST (Moonshot R&D) (Grant No. JPMJMS2061).

AUTHOR DECLARATIONS

Conflict of Interest

The authors have no conflicts to disclose.

Author Contributions

Takaaki Aoki: Conceptualization (lead); Data curation (lead); Formal analysis (lead); Investigation (lead); Methodology (lead); Software (lead); Validation (lead); Visualization (lead); Writing – original draft (lead); Writing – review & editing (equal). **Akiyoshi Tomonaga:** Conceptualization (supporting); Data curation (supporting); Formal analysis (supporting); Investigation (supporting); Methodology (supporting); Validation (supporting); Visualization (supporting); Writing – review & editing (equal). **Kosuke Mizuno:** Conceptualization (supporting); Data curation (supporting); Formal analysis (supporting); Investigation (supporting); Methodology (supporting); Validation (supporting); Visualization (supporting); Writing – review & editing (equal). **Shumpei Masuda:** Conceptualization (supporting); Data curation (supporting); Formal analysis (supporting); Investigation (supporting); Methodology (supporting); Project administration (lead); Supervision (lead); Validation (supporting); Visualization (supporting); Writing – original draft (supporting); Writing – review & editing (equal).

DATA AVAILABILITY

The data that support the findings of this study are available from the corresponding author upon reasonable request.

REFERENCES

- ¹P. T. Cochrane, G. J. Milburn, and W. J. Munro, *Phys. Rev. A* **59**, 2631 (1999).
- ²H. Goto, *Phys. Rev. A* **93**, 050301 (2016).
- ³S. Puri, S. Boutin, and A. Blais, *npj Quantum Inf.* **3**, 18 (2017).
- ⁴S. Puri, A. Grimm, P. Campagne-Ibarcq, A. Eickbusch, K. Noh, G. Roberts, L. Jiang, M. Mirrahimi, M. H. Devoret, and S. M. Girvin, *Phys. Rev. X* **9**, 041009 (2019).
- ⁵A. S. Darmawan, B. J. Brown, A. L. Grimsmo, D. K. Tuckett, and S. Puri, *PRX Quantum* **2**, 030345 (2021).
- ⁶N. E. Frattini, R. G. Cortiñas, J. Venkatraman, X. Xiao, Q. Su, C. U. Lei, B. J. Chapman, V. R. Joshi, S. M. Girvin, R. J. Schoelkopf, S. Puri, and M. H. Devoret, *Phys. Rev. X* **14**, 031040 (2024).
- ⁷S. Masuda, A. Yamaguchi, T. Yamaji, T. Yamamoto, T. Ishikawa, Y. Matsuzaki, and S. Kawabata, *New J. Phys.* **23**, 093023 (2021).
- ⁸A. Yamaguchi, S. Masuda, Y. Matsuzaki, T. Yamaji, T. Satoh, A. Morioka, Y. Kawakami, Y. Igarashi, M. Shirane, and T. Yamamoto, *New J. Phys.* **26**, 043019 (2024).
- ⁹I. García-Mata, R. G. Cortiñas, X. Xiao, J. Chávez-Carlos, V. S. Batista, L. F. Santos, and D. A. Wisniacki, *Quantum* **8**, 1298 (2024).
- ¹⁰J. Chávez-Carlos, T. L. M. Lezama, R. G. Cortiñas, J. Venkatraman, M. H. Devoret, V. S. Batista, F. Pérez-Bernal, and L. F. Santos, *npj Quantum Inf.* **9**, 76 (2023).
- ¹¹D. Ruiz, R. Gautier, J. Guillaud, and M. Mirrahimi, *Phys. Rev. A* **107**, 042407 (2023).
- ¹²J. Venkatraman, R. G. Cortiñas, N. E. Frattini, X. Xiao, and M. H. Devoret, *Proc. Natl. Acad. Sci.* **121**, e2311241121 (2024).
- ¹³B. Qing, A. Hajr, K. Wang, G. Koolstra, L. B. Nguyen, J. Hines, I. Huang, B. Bhandari, Z. Padramrazi, L. Chen, Z. Kang, C. Jünger, N. Goss, N. Jain, H. Kim, K.-H. Lee, A. Hashim, N. E. Frattini, J. Dressel, A. N. Jordan, D. I. Santiago, and I. Siddiqi, [arXiv:2411.04442](https://arxiv.org/abs/2411.04442) (2024).
- ¹⁴A. Cros Carrillo de Albornoz, R. G. Cortiñas, M. Schäfer, N. E. Frattini, B. Allen, D. G. A. Cabral, P. E. Videla, P. Khazaei, E. Geva, V. S. Batista, and M. H. Devoret, [arXiv:2409.13113](https://arxiv.org/abs/2409.13113) (2024).

- ¹⁵T. Kanao, S. Masuda, S. Kawabata, and H. Goto, *Phys. Rev. Appl.* **18**, 014019 (2022).
- ¹⁶S. Masuda, T. Kanao, H. Goto, Y. Matsuzaki, T. Ishikawa, and S. Kawabata, *Phys. Rev. Appl.* **18**, 034076 (2022).
- ¹⁷H. Chono, T. Kanao, and H. Goto, *Phys. Rev. Res.* **4**, 043054 (2022).
- ¹⁸H. Chono and H. Goto, [arXiv:2410.00552](https://arxiv.org/abs/2410.00552) (2024).
- ¹⁹T. Kanao and H. Goto, *Phys. Rev. Res.* **6**, 013192 (2024).
- ²⁰S. Puri, L. St-Jean, J. A. Gross, A. Grimm, N. E. Frattini, P. S. Iyer, A. Krishna, S. Touzard, L. Jiang, A. Blais, S. T. Flammia, and S. M. Girvin, *Sci. Adv.* **6**, eaay5901 (2020).
- ²¹Y.-H. Chen, R. Stassi, W. Qin, A. Miranowicz, and F. Nori, *Phys. Rev. Appl.* **18**, 024076 (2022).
- ²²Q. Xu, J. K. Iverson, F. G. S. L. Brandão, and L. Jiang, *Phys. Rev. Res.* **4**, 013082 (2022).
- ²³D. Iyama, T. Kamiya, S. Fujii, H. Mukai, Y. Zhou, T. Nagase, A. Tomonaga, R. Wang, J.-J. Xue, S. Watabe, S. Kwon, and J.-S. Tsai, *Nat. Commun.* **15**, 86 (2024).
- ²⁴D. Hoshi, T. Nagase, S. Kwon, D. Iyama, T. Kamiya, S. Fujii, H. Mukai, S. Ahmed, A. Frisk Kockum, S. Watabe, F. Yoshihara, and J.-S. Tsai, [arXiv:2406.17999](https://arxiv.org/abs/2406.17999) (2024).
- ²⁵A. Grimm, N. E. Frattini, S. Puri, S. O. Mundhada, S. Touzard, M. Mirrahimi, S. M. Girvin, S. Shankar, and M. H. Devoret, *Nature* **584**, 205 (2020).
- ²⁶A. Hajar, B. Qing, K. Wang, G. Koolstra, Z. Pedramrazi, Z. Kang, L. Chen, L. B. Nguyen, C. Jünger, N. Goss, I. Huang, B. Bhandari, N. E. Frattini, S. Puri, J. Dressel, A. N. Jordan, D. I. Santiago, and I. Siddiqi, *Phys. Rev. X* **14**, 041049 (2024).
- ²⁷M. Sarovar, T. Proctor, K. Rudinger, K. Young, E. Nielsen, and R. Blume-Kohout, *Quantum* **4**, 321 (2020).
- ²⁸Y. Chen, C. Neill, P. Roushan, N. Leung, M. Fang, R. Barends, J. Kelly, B. Campbell, Z. Chen, B. Chiaro, A. Dunsworth, E. Jeffrey, A. Megrant, J. Y. Mutus, P. J. J. O’Malley, C. M. Quintana, D. Sank, A. Vainsencher, J. Wenner, T. C. White, M. R. Geller, A. N. Cleland, and J. M. Martinis, *Phys. Rev. Lett.* **113**, 220502 (2014).
- ²⁹F. Yan, P. Krantz, Y. Sung, M. Kjaergaard, D. L. Campbell, T. P. Orlando, S. Gustavsson, and W. D. Oliver, *Phys. Rev. Appl.* **10**, 054062 (2018).
- ³⁰P. Mundada, G. Zhang, T. Hazard, and A. Houck, *Phys. Rev. Appl.* **12**, 054023 (2019).
- ³¹X. Li, T. Cai, H. Yan, Z. Wang, X. Pan, Y. Ma, W. Cai, J. Han, Z. Hua, X. Han, Y. Wu, H. Zhang, H. Wang, Y. Song, L. Duan, and L. Sun, *Phys. Rev. Appl.* **14**, 024070 (2020).
- ³²P. Zhao, P. Xu, D. Lan, J. Chu, X. Tan, H. Yu, and Y. Yu, *Phys. Rev. Lett.* **125**, 200503 (2020).
- ³³J. Ku, X. Xu, M. Brink, D. C. McKay, J. B. Hertzberg, M. H. Ansari, and B. L. T. Plourde, *Phys. Rev. Lett.* **125**, 200504 (2020).
- ³⁴J. Stehlík, D. M. Zajac, D. L. Underwood, T. Phung, J. Blair, S. Carnevale, D. Klaus, G. A. Keefe, A. Carniol, M. Kumph, M. Steffen, and O. E. Dial, *Phys. Rev. Lett.* **127**, 080505 (2021).
- ³⁵C. Leroux, A. Di Paolo, and A. Blais, *Phys. Rev. Appl.* **16**, 064062 (2021).
- ³⁶H. Goto, *Phys. Rev. Appl.* **18**, 034038 (2022).
- ³⁷P. Zhao, K. Linghu, Z. Li, P. Xu, R. Wang, G. Xue, Y. Jin, and H. Yu, *PRX Quantum* **3**, 020301 (2022).
- ³⁸F. Marxer, A. Vepsäläinen, S. W. Jolin, J. Tuorila, A. Landra, C. Ockeloen-Korppi, W. Liu, O. Ahonen, A. Auer, L. Belzane, V. Bergholm, C. F. Chan, K. W. Chan, T. Hiltunen, J. Hotari, E. Hyypää, J. Ikonen, D. Janzso, M. Koistinen, J. Kotilahti, T. Li, J. Luus, M. Papic, M. Partanen, J. Räbinä, J. Rosti, M. Savitskyi, M. Seppälä, V. Sevriuk, E. Takala, B. Tarasinski, M. J. Thapa, F. Tosto, N. Vorobeva, L. Yu, K. Y. Tan, J. Hassel, M. Möttönen, and J. Heinsoo, *PRX Quantum* **4**, 010314 (2023).
- ³⁹K. Kubo and H. Goto, *Appl. Phys. Lett.* **122**, 064001 (2023).
- ⁴⁰K. Kubo, Y. Ho, and H. Goto, *Phys. Rev. Appl.* **22**, 024057 (2024).
- ⁴¹T. Aoki, T. Kanao, H. Goto, S. Kawabata, and S. Masuda, *Phys. Rev. Appl.* **21**, 014030 (2024).
- ⁴²R. Narayan Rajmohan, A. Kenawy, and D. DiVincenzo, [arXiv:2201.01945](https://arxiv.org/abs/2201.01945) (2022).
- ⁴³H. Goto, *J. Phys. Soc. Jpn.* **88**, 061015 (2019).
- ⁴⁴P. Krantz, M. Kjaergaard, F. Yan, T. P. Orlando, S. Gustavsson, and W. D. Oliver, *Appl. Phys. Rev.* **6**, 021318 (2019).
- ⁴⁵S. Masuda, T. Ishikawa, Y. Matsuzaki, and S. Kawabata, *Sci. Rep.* **11**, 11459 (2021).
- ⁴⁶J. Chávez-Carlos, M. A. P. Reynoso, R. G. Cortiñas, I. García-Mata, V. S. Batista, F. Pérez-Bernal, D. A. Wisniacki, and L. F. Santos, *Quantum Sci. Technol.* **10**, 015039 (2025).
- ⁴⁷J. Johansson, P. Nation, and F. Nori, *Comput. Phys. Commun.* **183**, 1760–1772 (2012).
- ⁴⁸J. Johansson, P. Nation, and F. Nori, *Comput. Phys. Commun.* **184**, 1234–1240 (2013).
- ⁴⁹V. Gorini, A. Kossakowski, and E. C. G. Sudarshan, *J. Math. Phys.* **17**, 821 (1976).
- ⁵⁰G. Lindblad, *Commun. Math. Phys.* **48**, 119 (1976).
- ⁵¹N. E. Frattini, U. Vool, S. Shankar, A. Narla, K. M. Sliwa, and M. H. Devoret, *Appl. Phys. Lett.* **110**, 222603 (2017).
- ⁵²D. K. Tuckett, A. S. Darmawan, C. T. Chubb, S. Bravyi, S. D. Bartlett, and S. T. Flammia, *Phys. Rev. X* **9**, 041031 (2019).
- ⁵³J. P. Bonilla Ataides, D. K. Tuckett, S. D. Bartlett, S. T. Flammia, and B. J. Brown, *Nat. Commun.* **12**, 2172 (2021).